Second Order Model for Free Surface Convection

Seong-O. Kim*

자유표면유동을 위한 이차원 모델개발

김성오

VOF 방법에 의한 자유표면 유동계산의 정확성을 개선하기 위해 이차정도 모델을 개발하였다. 개발된 이차원 모델의 정확성을 비교하기 위하여 여러 가지 크기의 원형 및 Solitary wave형상의 자유표면 유동을 통하여 기존에 개발된 두 가지의 일차정도 모델과 비교하였다. 비교결과 반경이 큰 원과 같이 곡률이 작은 형상의 경우에는 일차정도 모델도 비교적 정확한 결과를 보여주고 있으나 작은 반경의 원형이나 Solitary wave와 같이 곡률이 큰 형상의 경우 일차정도 모델은 많은 오차를 보여주는 반면에 이차정도 모델은 어느 경우에나 매우 정확한 결과를 보여준다.

KEY WORDS: Volume-of-fluid: free surface flows: second-order model

1. Introduction:

Varieties of physical hydrodynamic phenomena involve interfaces between phases as shown Fig.1. The informations of the interfaces are necessary for solving the field equation such as mass and momentum equation. Up to now, various kinds of numerical method are developed to calculate the motion of the interfaces. One of the approaches is Lagrangian description of the interface in which the interfaces are calculated by tracing particles in Lagrangian method with the field variables calculated by Eulerian approach such as boundary integral technique[1], finite-element methods[2] and boundary-fitted coordinates[3]. This approach has simple logics but shows problem for large deformations of interface such as surface folding and breaks.

As an alternative approach, VOF(=volume of fluid) method can be applied to determine free surface curves by use of the VOF. The method is not susceptible to the problems

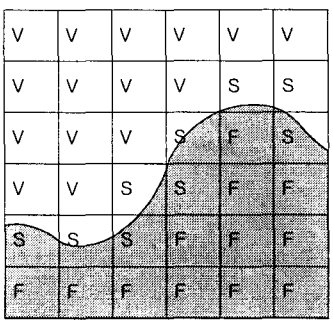

Fig. 1 Typical examples of free surface

which can be encountered when using the Lagrangian method.

In the earlier applications of the VOF method, donor-acceptor method with 0th-order[4] was used for VOF calculation, where the shape in a surface cell was assumed to be either horizontal or vertical rectangular shapes. For the calculation of VOF fluxes, the donor-acceptor method uses donor cell or acceptor cell alternatively based on the shape of donor cell to prevent over shooting or under shooting of VOF value. However the alternative usages of the donor

* 정회원, 한국원자력연구소

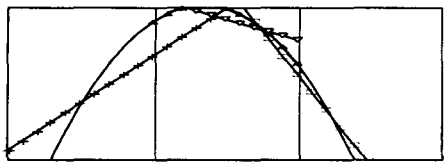

Fig. 2 The shapes of the reconstructed interface with large curvature by use of various free surface convection model.
—— :Analytic input data,
—⊟— :FLAIR method for the right
—|— :FLAIR method for the left
—▲— :Second-order method
—▽— :Centered slope method

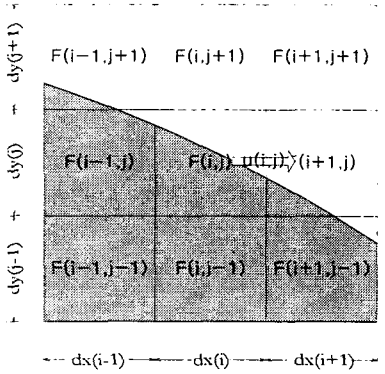

Fig. 3 Definition of cell block

or acceptor cell bring inaccurate results in VOF flux calculation. To improve the accuracy of free surface convection, two different approaches of the first-order method have been developed by Youngs[5] and Ashgriz[6]. The basic concept of the FLAIR method is to assume that the interfaces of a surface cell can be represented by a straight line with a slope determined at the face of two adjacent cells. On the other hand, Youngs' approach uses a slope in the cell center. But unfortunately, the detailed information of the method was not found in open literatures.

Even though the accuracy of VOF flux calculation is improved, the first-order methods make sharp edges near the end of a straight line as shown in Fig. 2. The sharp edge brings to generate flatsom which is one of reasons for the distortion of free surface and the total volume change of VOF. Therefore to improve accuracy of free surface convection a second-order approximation technique will be
developed in this study.

2. Second-order model

2.1 Slope calculation

The methodology applied for the second-order model is to find a second-order linear curve to fit the distribution of volume fraction. To calculate the slope at the face of a surface cell, it is assumed that the interface of free surface can be represented by either one of a single-valued function, f(x) or f(y), for the x, y directions. If the surface is represented as f(x), f(x) can be approximated as the sum of the volume fraction from cell (j-1) to cell (j+1) for each cell column of Fig. 3.:

$$f_i=\frac{\sum_{k=j-1}^{j+1}(dy_k F_{i,k})}{H}, \qquad H=\sum_{k=j-1}^{j+1} dy_k. \tag{1}$$

If the larger value of volume fraction between the two columns is assigned as F_M and the smaller one as F_m and the column width is represented as x_L(=L/H) for F_M and x_R(=R/H) for F_m, the boundary slope 'm' is calculated from equations (2), (3), (4) and (5).

Case-1:

$$m=\frac{2}{x_L^2}\left[-(2x_R F_m+x_L F_M)+2\sqrt{x_R F_m(x_R F_m+x_L F_M)}\right], \tag{2}$$

if $F_m \geq \frac{x_R F_M}{2x_R+x_L}$ and

$$x_L(1-F_M)+\sqrt{(F_m(1-F_M)x_L x_R)} \geq \frac{x_L}{2},$$

case-2:

$$m=\frac{2(F_m-F_M)}{(x_R+x_L)}, \tag{3}$$

if $F_m \geq \frac{x_R F_M}{2x_R+x_L}$, and

$$F_m \geq \frac{[F_M(x_R+2x_L)-(x_R+x_L)]}{x_L},$$

case-3:

$$\frac{1}{m} = -\{2[F_m x_R + \sqrt{F_m(1-F_M)x_R x_L}] + 2[(1-F_M)x_L + \sqrt{F_m(1-F_M)x_R x_L}]\}, \quad (4)$$

if $x_L(1-F_M)+\sqrt{(F_m(1-F_M)x_L x_R)} \leq \frac{x_L}{2}$

and $x_R f_m + \sqrt{f_m(1-f_M)x_R x_L} \leq \frac{x_R}{2}$,

case-4:

$$m = \frac{-2}{x_R^2}[2x_L(1-F_M)+x_R(1-F_m) + 2\sqrt{x_L(1-F_M)\{(x_L(1-F_M)+x_R(1-F_m)\}}\ ](5)$$

if $F_m \leq \frac{[F_M(x_R+2x_L)-(x_R+x_L)]}{x_L}$ and

$x_R F_m + \sqrt{F_m(1-F_M)x_R x_L} \geq \frac{x_R}{2}$.

2.2 Model case identification

A quadratic equation is defined as $y=a\cdot x^2+b\cdot x+c$ to represent the volume fraction distribution in a surface cell normalized by surface cell width W. The constants a and b are obtained by equation (6) for the case of unit cell width,

$$a=\frac{m_r-m_l}{2} \quad \text{and} \quad b=m_l. \quad (6)$$

When fitting the interface of a surface cell by the second-order curve, 8 possible shapes may exist as shown in Fig. 6.

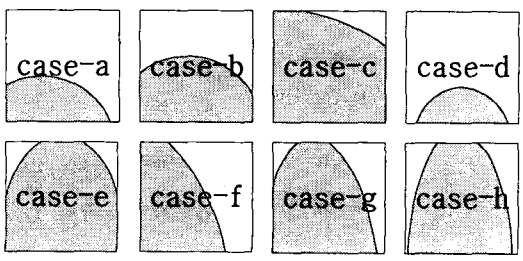

Fig. 4 Possible shapes of the interface in approximating the free surface by the second-order model

However, cases-f, g, h are excluded by adjusting the slope such that the maximum difference of volume fraction distribution lies within the cell height. The reason is that cases-f, g, h rarely appear in volume fraction calculation for the rearranged interface. Furthermore, higher than 4th order algebraic equations have to be solved to get the constant 'c' in the equation for the cases. Each case is identified by the equations (7)-(12).

Case-a

$$\text{if } F \geq \frac{m_l^3}{(m_l-m_r)^3} \text{ and } F \leq -\frac{(2m_r+m_l)}{6}, \quad (7)$$

case-b

$$\text{if } F \geq -\frac{(2m_r+m_l)}{6} \text{ and } F \leq 1-\frac{(m_l^3-m_r^3)}{(m_l-m_r)^2}, \quad (8)$$

case-c

$$\text{if } F \geq 1+\frac{(m_r+2m_l)}{6} \quad \text{for } m_l\cdot m_r \geq 0, \quad (9)$$

$$\text{if } F \geq 1+\frac{m_r-2m_l}{6}\left(\frac{m_r-m_l}{m_r+m_l}\right)^2 \quad \text{for } m_r\cdot m_l \leq 0, \quad (10)$$

case-d

$$\text{if } F \leq \frac{m_l^3}{6(m_r-m_l)^3}, \quad (11)$$

case-e

$$\text{if } F \geq 1-\frac{(m_l^3-m_r^3)}{(m_l-m_r)^2} \text{ and } F \leq 1+\frac{m_r-2m_l}{6}\left(\frac{m_r-m_l}{m_r+m_l}\right)^2. \quad (12)$$

2.3 Calculation of convective flux

To calculate the convective flux, the constant 'c' must be determined at first. For cases-b and d, the constant 'c' is determined explicitly by equations (13) and (14).

$$\text{for case-b,} \quad c=F-\frac{2m_r+m_l}{6}, \quad (13)$$

$$\text{for case-d,} \quad c=\frac{b^2}{4a}-\frac{a}{4}\left(-\frac{6F}{a}\right)^{2/3}. \quad (14)$$

However, for cases-a, c and e, the constant 'c' must be evaluated from the third order algebraic equation which comes from integrating the quadratic equation within the surface cell. After establishing the third-order

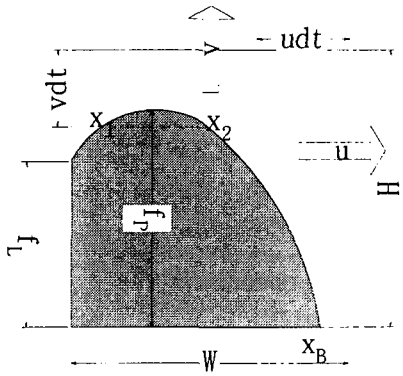

Fig. 5 Calculation of convective flux of second- order for each direction

algebraic equation, an appropriate solution is obtained by the Cardano's solution procedure[7].

The convective flux calculation in the second-order model is accomplished via integration of the quadratic equation from the cell face to the distance defined by the local velocity of the cell face over the time. For example, for case-a, the flux of volume fraction in the positive x direction is

$$\delta fx=0, \quad \text{if } x_P \geq x_B, \tag{15}$$

$$\delta fx=\int_{x_P}^{x_B} f dx, \quad \text{if } x_P \leq x_B, \tag{16}$$

where $x_P=1-u\cdot dt/W$.

The flux of VOF in the positive y direction is

$$\delta fy=0, \quad \text{if } y_P \geq f_F, \tag{17}$$

$$\delta fy=\int_{x_1}^{x_2}(f-y_P)dx, \quad \text{if } f_L \leq y_P \leq f_F, \tag{18}$$

$$\delta fy=\int_{0}^{x_2}(f-y_P)dx, \quad \text{if } y_P \leq f_P, \tag{19}$$

where $y_P=1-v\cdot dt/H$ and x_1, x_2 are the points where the second curve intersects the line $f=y_P$.

3. Results and discussion

3.1 Convection of circles

The second order model developed in this study is tested and compared with the FLAIR method and the centered slope method for the convection of circular geometry. Here,

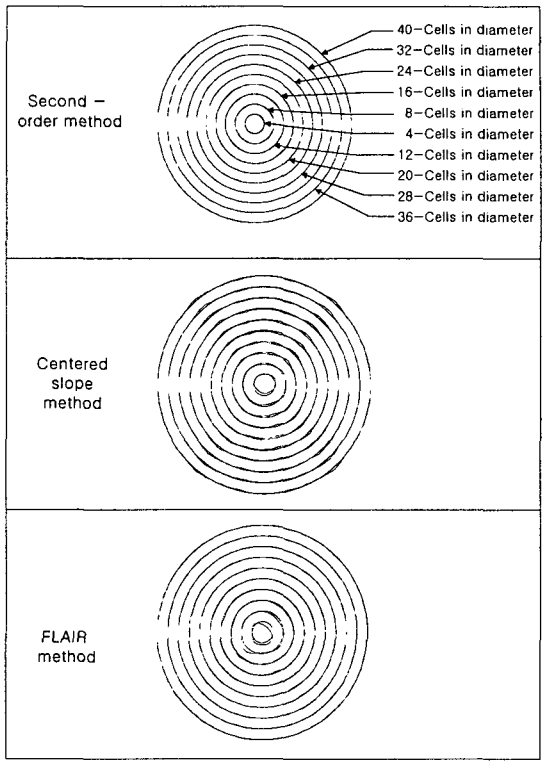

Fig. 6 Reconstruction of circles convected after 100 time steps by each free surface convection model

the convective calculations of free surface by FLAIR method are done with the program supplied by the original authors[6] which has large amounts of correction logic to prevent the diffusion of volume fraction. A uniform velocity field is assigned for the entire calculation region in the right and upward direction. The velocities in the x and y directions are one quarter of a uniform mesh size. Each circle is convected via this velocity for 100 time steps until all the circles completely move out of its original position. The calculation results are reviewed for three types of numerical errors. The first is a maximum cell error which can be an indication of local shape deformation. The second is the root of the square sum errors in every cell for indication of overall shape deformation. The final error is a total volume change to measure the conservation of volume fraction. The cell convection error is

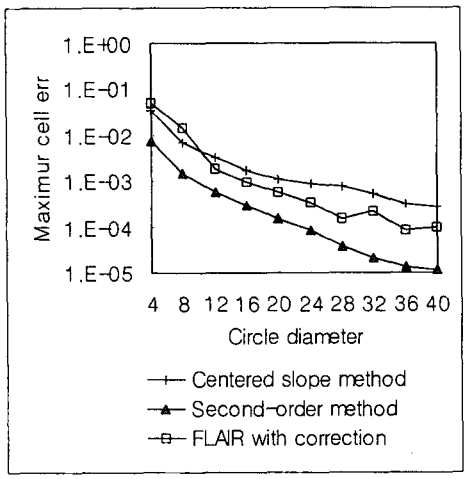

Fig. 7 Maximum cell error vs. circle diameter after 100 time step convections

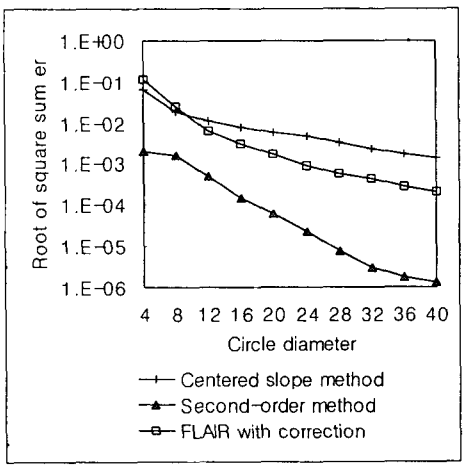

Fig. 8 Root of square sum error vs. circle diameter after 100 time step convections

normalized by circle area. To show the accuracy of the convection scheme of each technique, various sizes of concentric circles are drawn with the analytic circles in Fig. 6.

The shapes of free surface convected by the centered slope approach show a tendency toward a square edge. The shape given by the FLAIR method almost coincides with the analytic circle for large diameter. But when diameter is small the shape is seriously distorted. The shape given by the second-order method is almost identical to the analytic data.

The maximum cell error and the root of square sum error for each convection method are shown in Fig. 7 and Fig. 8. When comparing the errors between both of the first-order method, the FLAIR method gives smaller errors than the centered slope method for the circle with large diameter but the centered slope method gives smaller errors for the circle with small diameter. The results comes from the fact that when the diameter of a circle is large, the straight line constructed by the FLAIR method fit the interface correctly. On the other hand when the diameter of a circle is small, the FLIAR method yields a sharp edge. The sharp edge produce VOF convection errors from flatsom. However the second-order model always shows smaller error than both of the first-order method as shown Figs. 6,7. Further more, the second-order model with almost half the number of cells shows an equivalent magnitude of error as compared with both of the first-order approaches.

Both of the errors for each technique has similar tendency. This means that most of the cell convection error are very small except for the cells that have the dominant error.

The total volume change remains within order of 1.0E-6 for the first-order method and the second order method. However the FLAIR method shows the various amounts of volume change from the order of 1.0E-3 to the order of 1.0 of cell volume fraction for small sizes of diameter.

The total volume changes seems to come from the logic used in the FLAIR method to prevent from VOF overshoots and undershoots.

3.2 Convection of solitary waves

To compare the performance of the convection methods for a geometry with a sharp corner, solitary wave convection is

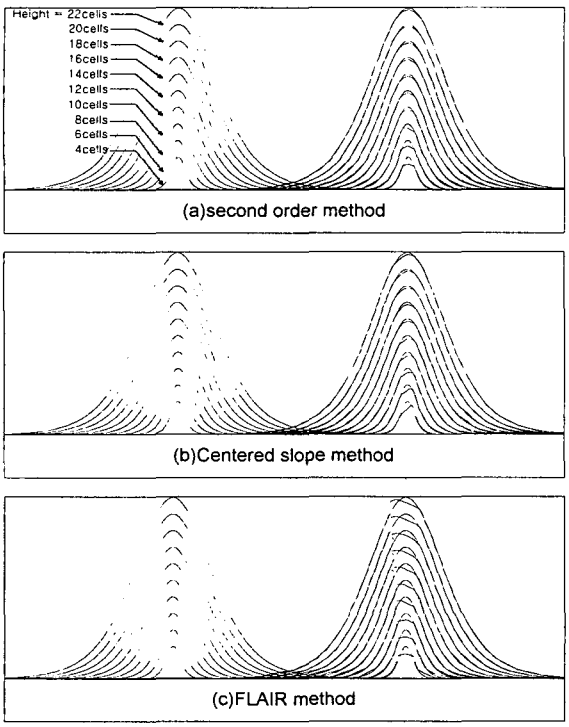

Fig. 9 Reconstruction of solitary wave convected after 100 time steps by each free surface convection model

examined which is represented in the form of $y=h\cdot \sec h^2(k\cdot x)+y_0$. As a sample case, the wave number k is assumed as 4.0/h and the wave height h varies from 4.0 to 16.0 times the cell length. The solitary wave is convected to the right hand direction with the uniform velocity in the x-direction as shown in Fig. 9.

After 100 convection time steps, the FLAIR method yields the worst results among the three approaches for both of errors (see Figs. 10 and 11). It may be reasoned that the FLAIR method produce inappropriate interface shape around the crest of wave as explained in section 3.1. As reviewing Figs. 10 and 11, the second-order method can reduce the number of meshes by half relative to the first-order method. Compared with the FLAIR method, the second-order method reduces the mesh number by factor of 2 to 3 times.

The total volume change remains

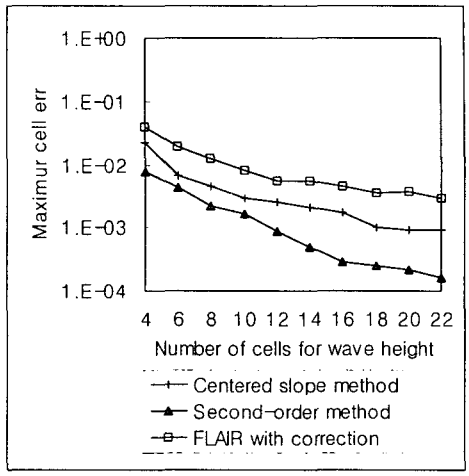

Fig. 10 Maximum cell error vs. solitary wave height after 100 time step convections

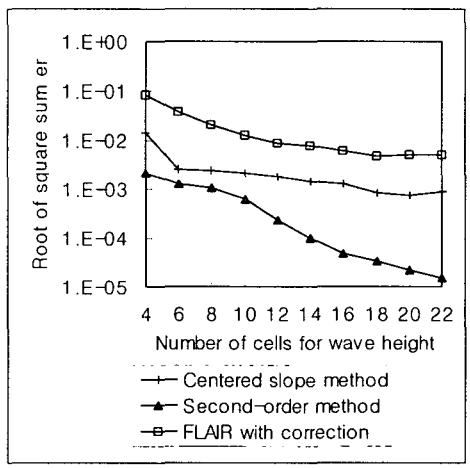

Fig. 11 Root of square sum error vs. solitary wave height after 100 time step convections

within order of 1.0E-6 for the first-order method and the second order method like the convection of circles. However the FLAIR method shows the various amounts of volume change from the order of 1.0E-3 to the order of 1.0 of cell volume fraction for small sizes of diameter

4. Conclusions

A new technique for the interface transport and reconstruction of the free surface was developed for the numerical

models of the volume fraction method by utilization of a set of second-order linear curves.

This technique was tested for the various sizes of circles and solitary waves advected with uniform velocities. For the small curvature of free surface such as a circle with a large diameter, both of the first-order approaches showed relatively close predictions compared with analytic solution. For large curvature geometry such as a circle with a relatively small diameter compared with the cell size or the solitary waves, the first-order approaches show the appreciable distortion of shape and diffusion of free surface. However, the second-order model consistently demonstrates accurate prediction of free surface convection even with a less number of cells.

However, the model developed in this study has been applied only for the surface with smooth interface. Therefore the application for a surface with sharp edge should be done after appropriate testing.

The second-order model has been developed for the 2-dimensional case but the model has a difficulty for directly extending to 3-dimensional case because the basic cases are increased and the algebraic calculations for VOF flux are much more complicated.

References

[1] H.C. Henderson, M. Kok and W.L. DE Koning, 'Computer-aided spillway design using the boundary element method and non-linear programming', Int. J. of Numer. Methods in Fluids, Vol.13, 625-641(1991).

[2] P. Bach and O. Hassager, 'An algorithm for the use of the Lagrangian specification in Newtonian fluid mechanics and applications to free-surface flow' J. of Fluid Mech. 152, 173-190 (1985).

[3] N.S. Asaithambi, 'Computation of free-surface flows', J. of Comput. Phys. 73, 380-394 (1987).

[4] C.W. Hirt and B.D. Nichols, 'Volume of Fluid(VOF) methods for the dynamics of free boundaries' J .of Comput. Phys. 39, 201-225 (1981).

[5] D.L. Youngs, Numerical methods for Fluid Dynamics, edited by K.W.Morton and M.J. Baines, Academic Press, New York, (1982).

[6] N. Ashgriz and J.Y. Poo, 'FLAIR (Flux Line-Segment Model for Advection and Interface Reconstruction' ,J. of Comput. Phys. 93, 449-468 (1991).

[7] Murray R. Spiegel, Mathematical handbook of formulas and tables in Schaum's outline series, (1968)ss

[8] Seong-O.Kim et. al, Second-Order Model for Free Surface Convection and Interface Reconstruction, KAERI/TR-836/97, 1997.3.